

Optimal power flow using archimedes optimizer algorithm

Mohammed Hamouda Ali¹, Ahmed Mohammed Attiya Soliman¹, Salah K. Elsayed²

¹Department of Electrical Engineering, Faculty of Engineering, Al-Azhar University, Cairo, Egypt

²Department of Electrical Engineering, College of Engineering, Taif University, Taif, Saudi Arabia

Article Info

Article history:

Received Apr 6, 2022

Revised May 23, 2022

Accepted June 11, 2022

Keywords:

Archimedes optimization algorithm
Metaheuristic algorithms
Multi-objective functions
Optimal power flow
Renewable energy source

ABSTRACT

This article proposes a new metaheuristic algorithm called Archimedes optimization algorithm (AOA) for solving optimization problems of optimal power flow (OPF) utilizing the renewable energy sources (RES) for minimizing different single-objective and multi-objective functions based on minimization of fuel cost, power losses of transmission lines, emission and voltage profile improvement. Also, mathematical formulation of (OPF) is introduced by converting the function with multiple objectives based on price and weighting parameters into a single objective function. Also, the effect of optimal RES is merged into the OPF problem. Notably, optimal RES placement yields even more effective solution. AOA was inspired by an intriguing physical law known as Archimedes' Principle. To prove the effectiveness of the AOA proposed algorithm, it compared with different recent algorithms for solving the optimal power flow problems and testing them to one standard system of the IEEE30-bus test system. The superiority of the proposed AOA algorithm is proven also by applying them on the IEEE30-bus modified system with optimal allocation of renewable energy source (RES). The results demonstrate that the proposed algorithm is more successful and efficient than the other optimization methods in the title of resolving OPF problems.

This is an open access article under the [CC BY-SA](https://creativecommons.org/licenses/by-sa/4.0/) license.



Corresponding Author:

Mohammed Hamouda Ali

Department of Electrical Engineering, Faculty of Engineering, Al-Azhar University

P.O. Box 11751, El Nasr St, Nasr City, Cairo, Egypt

Email: Eng_MohammedHamouda@azhar.edu.eg, MohammedHamouda62.el@azhar.edu.eg

1. INTRODUCTION

The term "optimal power flow" (OPF) refers to the operation of a power system in an economical and stable manner, which is achieved by properly setting the system's control variables, where (OPF) is a critical and nonlinear complex optimization problem for assessing security and dependability of power systems, whose primary goal is to select the optimal network or grid control variable solution that fulfils the minimal objective function value while taking system constraints into consideration. where OPF aims to optimize generator dispatch based on their limits, expected operating conditions, voltage constraints on the bus, as well as safety margins [1], [2]. Many control variables, including generator voltage, generator actual output power, transformer tap settings, and reactive power compensation devices, can be used in this situation. Renewable energy sources (RES), specifically wind turbines and solar generators, have recently been recommended for due to clean energy production and reducing operating costs. The allocation and technical characteristics of renewable energy generators have a significant impact on the system's techno-economic performance [1]–[5]. As a result, control variables, generator behaviour, and the establishment of an accurate planning tool for optimal power flow in the integrated electric system [1]–[7] must be considered.

An objective function definition should be used to pick the optimal solution as the desired solution. Different objectives for the OPF are considered in the electrical system. As a result, the optimal power flow takes system constraints into account and determines the most optimal operating conditions in terms of both system control variables, and objectives of the problem. OPF's optimal solution has been linked with technical and economical benefits, which are typically regarded to be OPF objectives. Generally, the objective functions of OPF may be divided into single objective functions that achieve a single goal and multi-objective functions that achieve many objectives at the same time. These objectives might include the generators fuel cost, emission rate of the generator, the power losses in an electric network, and security index of the voltage [1]–[7]. As presented in [8]–[10], many optimization methods have been devised for solve the OPF issues. These methods may be divided into two categories: conventional methods and metaheuristics methods as presented in [9]. To address the OPF problems, several traditional approaches were being used, including linear programming [11], nonlinear programming [12], quadratic programming [13], newton method network flow programming [14], as well as the interior point technique [15]. The primary drawbacks of traditional approaches are that they are unsuitable for large and complex OPF problems, which are non-linear and multi-modality optimization issues, as a result of the significant sophistication and nonlinear effects of the restricted OPF issue, it has been revealed that conventional techniques may not even be capable of handling the OPF problem solutions correctly, resulting in poor results [3], [9].

According to the literature survey in [3], [9] various metaheuristic optimization approaches including evolutionary-inspired, bio-inspired, human-inspired, physics-inspired, hybrid, swarm and artificial neural networks-fuzzy logic approaches, these approaches are invented and proposed to fill the gap formed by the use of conventional methods and getting the best optimum solutions when dealing with OPF difficult issues. Furthermore, the incorporation of new renewable sources, particularly WT and PV, into the power system adds complexity of the OPF problem due to their intermittent power generation characteristics. As a result, to fill the gap left by the use of conventional methods, a comprehensive overview of various metaheuristic optimization approaches for the optimal solution of power flow issues has been invented and proposed [3], [9]. Finally, when compared to traditional techniques, the advantages of these metaheuristic techniques include high dependability, guaranteed best optimized solution, rapid convergence, and a low likelihood of errors and being trapped in local minima. Because of the optimal outcomes, most researchers in recent study work considered a metaheuristic population-based approach to resolving the OPF issue.

Several research articles used nature-inspired techniques for solving the OPF problems. Jadhav and Bamane [16] solve the problem of OPF with a single objective function and employed the best-guided algorithm called artificial bee colony to optimize the fuel cost. Glow-worm swarm optimization algorithm is used to optimize emission and fuel cost as in [17]. Tan *et al.* [18] the fuel cost is optimized with only valve effect by using the improved group search optimization algorithm. Power losses, fuel cost, fuel cost with valve effect, emission are optimized in [19] employed the oppositional krill herd algorithm. Also, algorithm known as chaotic artificial bee colony is used to optimize transient stability and fuel cost as in [20]. Also, Mukherjee and Mukherjee [21] solve the OPF problem and employed the chaotic krill herd algorithm to optimize fuel cost, fuel cost with valve effect, emission, power losses, and voltage deviation. Mohamed *et al.* [22] solving the OPF problems with multi-objective function and employed algorithm called moth swarm to optimize emission, fuel cost, fuel cost with only valve effect, L-index, power losses, piecewise cost, and voltage deviation.

Several research articles used the algorithms inspired by humans that were used for solving the OPF problems. Where improved harmony search algorithm is employed in [23] to solve OPF problem using only single objective function and optimize the fuel cost only with valve effect. Also, fuel cost, fuel cost considering the banned regions, and fuel cost with valve effect have been optimised in [24] using algorithm called symbiotic organisms search. Adaryani and Karami [25] fuel cost with only valve effect and emission based on using the modified teaching-learning algorithm are optimized. Ghasemi *et al.* [26] solve the OPF problem and employed algorithm known as the improved teaching-learning to optimize fuel cost, fuel cost with only valve effect, emission, piecewise cost, and voltage deviation. Mandal and Roy [27] employed optimization algorithm known as quasi-oppositional teaching learning algorithm to optimize emission, fuel costs with valve effect, L-index, power losses, and L-index.

Many research papers applied evolutionary-based optimization techniques for solving the OPF problem. Somasundaram *et al.* [28] authors are solving the optimal power flow problem with a single objective function and employed the evolutionary programming algorithm to optimize the fuel cost. A faster algorithm called evolutionary is applied in [29] to optimize fuel cost and fuel cost with only valve effect. Optimizing of fuel cost and emission is presented in [30] by using the improved evolutionary algorithm. Power losses, fuel cost, emission, and L-index are optimized in [31] employed enhanced self-adaptive differential evolution. Reddy and Bijwe [32], differential evolution algorithm is applied to optimize power losses, L-index, fuel cost, and fuel cost with only valve effect. Chaib *et al.* [33] solve the OPF problem and employed the backtracking search method to optimize emission, L-index, fuel cost, fuel cost with only valve effect, piecewise cost, and voltage deviation.

Several research articles present the applicable physics-inspired techniques for solving the OPF issues. Boucekara *et al.* [34], the author solved the OPF problem with multi-objective function and employed optimization method called an improved colliding bodies to optimize emission, fuel cost, fuel cost with only valve effect, L-index, power losses, voltage deviation, and piecewise cost. Many research papers discuss composite optimization techniques that have been used for OPF. Gacem and Benattous [35] used particle swarm and genetic algorithm to optimize fuel cost, and cost of fuel with valve effect. Fuel cost, cost of fuel with valve effect, emission, L-index, piecewise cost, and voltage deviation is optimized in [36] by employing Nelder-Mead and fuzzy particle swarm optimization algorithms. Also, Singh *et al.* [37] with an aging leader and challengers employed particle swarm optimization algorithm to optimize fuel cost, fuel cost with only valve effect, voltage deviation, and power losses. The optimizations techniques based on ANNs and fuzzy logic approaches are presented through several research articles as in references [38]-[40].

To summarise, this article presents a new population-based algorithm called archimedes optimization algorithm (AOA) based on the physics law known as Archimedes' principle to compete with state-of-the-art and recent optimization algorithms, including other physics-inspired methods. It is important to note that the proposed technique strikes a balance between exploration and exploitation. Because AOA keeps a population of solutions and investigates a large area to find the best global solution, it is well suited for solving complex optimization problems with many locally optimal solutions. In conclusion, the following are the main contributions of this research:

- Archimedes optimization algorithm (AOA) has been proposed as a new population-based algorithm that mimics Archimedes' principle.
- Introduce the OPF problem formulation with different four objective-functions.
- Applying the proposed AOA for solving the optimization problems by converting the multi-objective function (fuel cost, power losses, voltage deviation, and emission) into a single-objective function using the price and weighting factors.
- The IEEE30-bus testing system is used in this study to assess the effect of the proposed algorithm on a difficult test suite in metaheuristic literary works.
- The search efficiency of AOA is validated against well-established algorithms dragonfly algorithm (DA), particle swarm optimization (PSO), sparrow search algorithm (SSA), future search algorithm (FSA).
- The AOA algorithm is also proposed for deciding the best and optimal allocation of RES.
- Finally, the modified IEEE30-bus testing system integrated with the optimal RES allocation is introduced to test the AOA suggested algorithm's supremacy over other metaheuristic algorithms.

This paper organization is as follows: section 2 introduces the mathematical formulation model of the OPF. The AOA proposed algorithm is discussed in section 3. Also, section 4 contains the AOA simulation results. In this section, a thorough analysis and comparison are performed against the selected metaheuristic algorithms. Section 5 presents the final discussion and conclusion.

2. MATHEMATICAL FORMULATION FOR OPF

The optimum power flow issue seeks to maximize an objective function by making optimal modifications to the control variables of power system while adhering to various equality constraints and inequality constraints. In general, the optimization issue may be mathematically stated as:

$$\min F(x, u) \quad (1)$$

Conditional on:

$$g_j(x, u) = 0 \quad j = 1, 2, \dots, m$$

$$h_j(x, u) \leq 0 \quad j = 1, 2, \dots, p$$

Where function F represents the objective function, x is a vector containing the state variables (dependent variables), u is a vector containing the control variables (independent variables), and g_j and h_j are respectively the equality and inequality requirements. The variables m and p represent respectively the equality and inequality constraints numbers. In a power system, the state variables (x) are as:

$$x = [P_{G1}, V_{L1} \dots V_{L, NPQ}, Q_{G,1} \dots Q_{G, NG}, S_{TL,1} \dots S_{TL, NTL}] \quad (2)$$

where P_{G1} denotes power of slack bus, V_L denotes load bus voltage, Q_G denotes reactive output power for generator, S_{TL} denotes the transmission line's apparent power flow, NPQ denotes the load buses number, NG denotes the generation buses number, and NTL denotes the transmission lines number. In a power system, the control variables (u) are as:

$$u = [P_{G,2} \dots P_{G,NG}, V_{G,1} \dots V_{G,NG}, Q_{C,1} \dots Q_{C,NC}, T_1 \dots T_{NT}] \quad (3)$$

where P_G is the active output power for generator, V_G is the generation bus voltage, Q_C is the shunt compensator reactive power injected, T is the tap setting for transformer, NC is the shunt compensator units number, and NT is the transformers number.

2.1. Objective functions

An objective function definition should be used to pick the optimal solution as the desired solution. In addition to the problem objectives, different objectives are assessed for the OPF, going to result in an optimized power flow that considers system constraints and determines the finest conditions in terms of system control variables, in furthermore to the problem objectives. OPF's best solution has been linked to techno-economic advantages, which are commonly referred to as OPF objectives. Reduced fuel costs in terms of annual savings are among the economic benefits, while the technical benefits are listed [3]:

- Minimization of active power losses
- Minimization of reactive power losses
- System reliability, and power quality enhancement
- Deviation of the voltage
- Stability of the voltage

2.1.1. Single objective functions

A most common objective-functions can be performed as follows [41]-[45]:

- Basic fuel costs minimization objective

This objective function is the primary aim of the OPF issue and seeks to minimize overall fuel cost. For every generator, it may be demonstrated as a quadratic polynomial function as:

$$F_1 = \sum_{i=1}^{NG} F_i(P_{Gi}) = \sum_{i=1}^{NPV} (a_i + b_i P_{Gi} + c_i P_{Gi}^2) \frac{\$}{h} \quad (4)$$

where, F_i is the i th generator fuel cost. a_i , b_i , and c_i are the cost coefficients for i th generator.

- Generation emission minimization objective

Reducing the amount of gas emitted by thermal power plants can help to reduce pollution. The objective function for the emission gases is as:

$$F_2 = \sum_{i=1}^{NG} (\gamma_i P_{Gi}^2 + \beta_i P_{Gi} + \alpha_i + \zeta_i \exp(\lambda_i P_{Gi})) \quad (5)$$

where, γ_i , β_i , α_i , ζ_i , and λ_i are the i th generator's emission coefficients.

- Active power losses minimization objective

The desired objective-function is to minimize real power loss, which can be presented as:

$$F_3 = \sum_{i=1}^{NTL} G_{ij} (V_i^2 + V_j^2 - 2 V_i V_j \cos \delta_{ij}) \text{ MW} \quad (6)$$

where, G_{ij} the transmission conductance, NTL is the transmission lines number, and δ_{ij} is the voltages phase difference.

- Voltage profile improvement

The deviations of load buses voltage from a predetermined voltage are minimized by this objective function, it may be expressed as:

$$F_4 = VD = \sum_{i=1}^{NPQ} |V_i - 1| \quad (7)$$

2.1.2. Multi-objective functions

The primary goal of resolving a multi-objective problem is to optimize multiple independent objective functions simultaneously and its definition is represented as:

$$\text{Min } F(x, u) = [F_1(x, u), F_2(x, u), \dots, F_i(x, u)] \quad (8)$$

where i is the objective functions number, the optimization with Pareto approach or weight factors as follows can be used to solve multi objective functions:

$$\begin{aligned} \text{Min } F_5 &= \sum_{i=1}^4 w_i F_i(x, u) \\ F(x, u) &= w_1 F_1 + w_2 F_2 + w_3 F_3 + w_4 F_4 \end{aligned} \quad (9)$$

$$F(x, u) = w_1 \sum_{i=1}^{NG} (a_i + b_i P_{Gi} + c_i P_{Gi}^2) + w_2 \sum_{i=1}^{NG} (\gamma_i P_{Gi}^2 + \beta_i P_{Gi} + \alpha_i + \zeta_i \exp(\lambda_i P_{Gi})) + w_3 \sum_{i=1}^{NTL} G_{ij} (V_i^2 + V_j^2 - 2 V_i V_j \cos \delta_{ij}) + w_4 \sum_{i=1}^{NPQ} |V_i - 1| \quad (10)$$

where w_1 , w_2 , w_3 and w_4 are weight factors chosen based on the relative importance of one goal to another. Typically, the values of the weight factors are chosen as:

$$\sum_{i=1}^n w_i = 1 \quad (11)$$

2.2. System constraints

There are already many constraints in the system that can be classified as:

2.2.1. The Equality constraints

The equality constraints for the balanced load flow equations are as:

$$P_{Gi} - P_{Di} = |V_i| \sum_{j=1}^{NB} |V_j| (G_{ij} \cos \delta_{ij} + B_{ij} \sin \delta_{ij}) \quad (12)$$

$$Q_{Gi} - Q_{Di} = |V_i| \sum_{j=1}^{NB} |V_j| (G_{ij} \sin \delta_{ij} - B_{ij} \cos \delta_{ij}) \quad (13)$$

where P_{Gi} and Q_{Gi} are the active power and reactive power generated respectively at bus i , the active and reactive demand of the load at bus i are represented by P_{Di} and Q_{Di} , respectively. G_{ij} and B_{ij} represent conductance and susceptance among buses i and j , respectively.

2.2.2. Inequality constraints

The Inequality constraints is categorized as:

$$\text{Active output power of generators } P_{Gi}^{\min} \leq P_{Gi} \leq P_{Gi}^{\max} \quad i = 1, 2, \dots, NG \quad (14)$$

$$\text{Voltages at generators buses } V_{Gi}^{\min} \leq V_{Gi} \leq V_{Gi}^{\max} \quad i = 1, 2, \dots, NG \quad (15)$$

$$\text{Reactive output power of generators } Q_{Gi}^{\min} \leq Q_{Gi} \leq Q_{Gi}^{\max} \quad i = 1, 2, \dots, NG \quad (16)$$

$$\text{Tap settings of transformer } T_i^{\min} \leq T_i \leq T_i^{\max} \quad i = 1, 2, \dots, NT \quad (17)$$

$$\text{Shunt VAR compensator } Q_{Ci}^{\min} \leq Q_{Ci} \leq Q_{Ci}^{\max} \quad i = 1, 2, \dots, NC \quad (18)$$

$$\text{Apparent power flows in transmission lines } S_{Li} \leq S_{Li}^{\max} \quad i = 1, 2, \dots, NTL \quad (19)$$

$$\text{Magnitude of load buses voltage } V_{Li}^{\min} \leq V_{Li} \leq V_{Li}^{\max} \quad i = 1, 2, \dots, NPQ \quad (20)$$

The dependent control variables can be easily incorporated into an optimization solution by using the quadratic penalties formulation of the objective-function, which is stated:

$$F_g(x, u) = F_i(x, u) + K_G (\Delta P_{G1})^2 + K_Q \sum_{i=1}^{NPV} (\Delta Q_{Gi})^2 + K_V \sum_{i=1}^{NPQ} (\Delta V_{Li})^2 + K_S \sum_{i=1}^{NTL} (\Delta S_{Li})^2 \quad (21)$$

where K_G , K_Q , K_V , and K_S are penalty factors with large positive values, also ΔP_{G1} , ΔQ_{Gi} , ΔV_{Li} , and ΔS_{Li} are penalty conditions that can be stated as:

$$\Delta P_{G1} = \begin{cases} (P_{G1} - P_{G1}^{\max}) & P_{G1} > P_{G1}^{\max} \\ (P_{G1} - P_{G1}^{\min}) & P_{G1} < P_{G1}^{\min} \\ 0 & P_{G1}^{\min} < P_{G1} < P_{G1}^{\max} \end{cases} \quad (22)$$

$$\Delta Q_{Gi} = \begin{cases} (Q_{Gi} - Q_{Gi}^{\max}) & Q_{Gi} > Q_{Gi}^{\max} \\ (Q_{Gi} - Q_{Gi}^{\min}) & Q_{Gi} < Q_{Gi}^{\min} \\ 0 & Q_{Gi}^{\min} < Q_{Gi} < Q_{Gi}^{\max} \end{cases} \quad (23)$$

$$\Delta V_{Li} = \begin{cases} (V_{Li} - V_{Li}^{max}) & V_{Li} > V_{Li}^{max} \\ (V_{Li} - V_{Li}^{min}) & V_{Li} < V_{Li}^{min} \\ 0 & V_{Li}^{min} < V_{Li} < V_{Li}^{max} \end{cases} \quad (24)$$

$$\Delta S_{Li} = \begin{cases} (S_{Li} - S_{Li}^{max}) & S_{Li} > S_{Li}^{max} \\ (S_{Li} - S_{Li}^{min}) & S_{Li} < S_{Li}^{min} \\ 0 & S_{Li}^{min} < S_{Li} < S_{Li}^{max} \end{cases} \quad (25)$$

3. ARCHIMEDES OPTIMIZATION ALGORITHM OVERVIEW

AOA mimics the concept of the force of buoyancy which imposed upwards to an object partially or completely immersed in fluid, proportional to the weight of the displaced fluid. AOA is a population-based algorithm, and the individuals in the population are the immersed objects in the proposed approach. AOA, like other population-based metaheuristic algorithms, begins the search process by populating objects (candidate solutions) with random volumes, densities, and accelerations. At this point, each object is also given a random position in fluid. AOA works in iterations until the termination condition is met after evaluating the fitness of the initial population. AOA updates the density and volume of each object in each iteration. The object's acceleration is updated based on the condition of its collision with any other neighboring object. The new position of an object is determined by the updated density, volume, and acceleration. The detailed mathematical formulation of AOA steps is given.

3.1. Algorithmic steps

The mathematical formulation of the AOA algorithm is introduced in this section. AOA, in theory, can be thought of as a global optimization algorithm because it encompasses both exploration and exploitation processes. Algorithm 2 shows the proposed algorithm's pseudo-code, which includes population initialization, population evaluation, and parameter updating. The steps of the AOA are detailed mathematically as follows.

- Step 1: Initialization

Initialize the positions of all objects using (26):

$$O_i = lb_i + rand \times (ub_i - lb_i); i = 1, 2, \dots, N \quad (26)$$

where O_i is the object i_{th} in a population of N objects, lb_i and ub_i are respectively the lower and the upper bounds of the search-space. Density (den) and initial volume (vol) and for each object i_{th} using (27) and (28):

$$den_i = rand \quad (27)$$

$$vol_i = rand \quad (28)$$

where $rand$ is a D-dimensional vector that generates a number at random between [0, 1]. Finally, initialize acceleration (acc) of object i_{th} using (29):

$$acc_i = lb_i + rand \times (ub_i - lb_i) \quad (29)$$

inside this step, assess the initial population and choose the object with the highest fitness value. Assign x_{best} , den_{best} , vol_{best} , and acc_{best} .

- Step 2: Update densities, volumes

The density and volume of i object for the iteration $t + 1$ is updated using (30) and (31):

$$den_i^{t+1} = den_i^t + rand \times (den_{best} - den_i^t) \quad (30)$$

$$vol_i^{t+1} = vol_i^t + rand \times (vol_{best} - vol_i^t) \quad (31)$$

where vol_{best} and den_{best} are the volume and density affiliated with the finest object discovered thus far, and $rand$ is an uniform random number.

- Step 3: Transfer operator and density factor

Initially, objects collide, and after a period, the objects attempt to reach an equilibrium state. This is accomplished in AOA using the transfer factor TF , which transforms search from exploration to exploitation, as defined by (32).

$$TF = \exp\left(\frac{t-t_{max}}{t_{max}}\right) \quad (32)$$

Where the transfer TF gradually increases over time until it reaching 1. Here t and t_{max} are iteration number and maximum number of iterations, respectively. Similarly, the density decreasing factor d also aids in its global to local search. It decreases over time when using (33).

$$d^{t+1} = \exp\left(\frac{t-t_{max}}{t_{max}}\right) - \left(\frac{t}{t_{max}}\right) = TF - \left(\frac{t}{t_{max}}\right) \quad (33)$$

Where d^{t+1} decreases over time, allowing convergence in a previously identified outstanding region. It should be noted that proper handling of this variable will ensure AOA's balance of exploration and exploitation.

- Step 4.1: Exploration phase (collision between objects occurs)

If $TF \leq 0.5$, an object collides, choose a random material (mr) and update acceleration of the object for iteration $t + 1$ using (34):

$$acc^{t+1} = \frac{den_{mr} + vol_{mr} \times acc_{mr}}{den_i^{t+1} \times vol_i^{t+1}} \quad (34)$$

where den_i , vol_i , and acc_i are density, volume, and acceleration of i object. Besides that, acc_{mr} , den_{mr} and vol_{mr} are the acceleration, density, and volume of random material. It is worth noting that $TF \leq 0.5$ guarantees exploration during one-third of iterations. Changing the value from 0.5 to something else will alter the exploration-exploitation behavior.

- Step 4.2: Exploitation phase (no collision between objects)

If $TF > 0.5$, Objects do not collide, update acceleration of the object for iteration $t + 1$ using (35):

$$acc^{t+1} = \frac{den_{best} + vol_{best} \times acc_{best}}{den_i^{t+1} \times vol_i^{t+1}} \quad (35)$$

Where acc_{best} is the acceleration of the best object.

- Step 4.3: Normalize acceleration

Normalize acceleration to calculate the percentage of change using (36).

$$acc_{i-norm}^{t+1} = u \times \frac{acc_i^{t+1} - \min(acc)}{\max(acc) - \min(acc)} + l \quad (36)$$

Where u and l are the range of normalization and set to 0.9 and 0.1, respectively. The acc_{i-norm}^{t+1} determines how much each agent will change in one step. If the object I is very far from the global optimum, the acceleration value will be high, indicating that it is in the exploration phase; or else, it is in the exploitation phase. This diagram depicts how the search progresses from the exploratory to the exploitation phase. In most cases, the acceleration factor starts out high and gradually decreases. These assists search agents in moving away from local solutions and toward the best solution globally. However, it is worth noting that some search agents may require more time to remain in the exploration phase than usual. As a result, AOA achieves the desired balance of exploration and exploitation.

- Step 5: Update position

If ($TF \leq 0.5$) means less than 0.5 (exploration phase), the i_{th} position of the object for next iteration $t + 1$ using (37):

$$x_i^{t+1} = x_i^t + C_1 \times rand \times acc_{i-norm}^{t+1} \times d \times (x_{rand} - x_i^t) \quad (37)$$

where C_1 is a constant equals to 2. Otherwise, if ($TF > 0.5$) means greater than 0.5 (exploitation phase), the objects' positions are updated using (38):

$$x_i^{t+1} = x_{best}^t + F \times C_2 \times rand \times acc_{i-norm}^{t+1} \times d \times (T \times x_{best} - x_i^t) \quad (38)$$

where C_2 a fixed value of 6. T grows with time, is proportional to the transfer operator, and is defined using $T = C_3 \times TF$. T increases with time in range $[C_3 \times 0.3, 1]$ and initially deducts a certain percentage from the best position. It begins with a low percentage because this results in a large difference between the best and current positions; as a result, the step-size of the random walk will be large. As the search progresses, this

percentage gradually increases to reduce the gap between the best and current positions. This results in an appropriate balance of exploration and exploitation. F is the flag to change the direction of motion using (39):

$$F = \begin{cases} +1 & \text{if } P \leq 0.5 \\ -1 & \text{if } P > 0.5 \end{cases} \quad (39)$$

where, $P = 2 \times rand - C_4$.

- Step 6: Evaluation

Evaluate every object using the objective function f , and keep the best solution found so far in mind. Assign x_{best} , den_{best} , vol_{best} , and acc_{best} .

3.2. AOA-based optimization process

This paper's holistic optimization model includes multi-dimensional parameters. The main AOA encoding is no longer applied. The code vector for comprehensive OPF optimization is as:

$$[P_{G2}, P_{G5}, P_{G8}, P_{G11}, P_{G13}, V_1, V_2, V_5, V_8, V_{11}, V_{13}, T_{11}, T_{12}, T_{15}, T_{36}, Q_{10}, Q_{12}, Q_{15}, Q_{17}, Q_{20}, Q_{21}, Q_{23}, Q_{24}, Q_{29}]$$

4. RESULTS OF SIMULATION

To investigate the efficacy of using AOA to resolve the OPF issue, it is investigated using one standard test system of IEEE-30 bus test system. In this section, the simulation results of solving OPF using AOA are compared to those obtained by other recent metaheuristic algorithms. The potential of AOA to minimize the fuel cost, active power loss, total deviation in the voltage, and emission as a single-objective problem for each objective and as a multi objective problem using weight factors which evaluated based on the following cases presented below. Also, he proposed AOA algorithms' efficiency is also tested against other algorithms through the modified IEEE30-bus test system to introduce the optimal allocation for RES and prove its validity with minimizing of the fuel cost. The appropriate parameters of the AOA and other methods are chosen based on empirical tests through running these algorithms considerable many times for the test system with combination of different parameters. The application of AOA and other compared techniques to solve OPF problem have been run on, a I7-8700 CPU, 16 GB RAM PC 2.8GHz, and MATLAB 2018a.

4.1. Testing system description.

The standard IEEE 30-bus test system includes 6 generation power units, 41 lines and 24 load buses. Bus no. 1 is selected as slack bus. The active and reactive power values of the total connected load are 2.834 pu and 1.262 pu, respectively. The voltage magnitude of the power generating buses is limited between 0.95 pu and 1.1 pu, while the voltage magnitude of the remaining load buses is limited between 0.95 pu and 1.05 pu. Furthermore, the tap changing transformers are adjustable between 0.9 and 1.1 pu. Furthermore, the VAR compensator limit is set to fluctuate between 0 and 0.05 pu. Finally, more information about all of the buses and lines data of the IEEE 30-bus testing system can be found and described in [46]-[48].

4.1.1. Case1: Minimization of fuel cost

The proposed AOA in this case is implemented on the IEEE 30-bus test system to reduce fuel costs. Table 1 shows the best results obtained by the AOA as well as those obtained by other reported algorithms in the literature. such as FSA, SSA, PSO [49] and DA [50]. According to the simulated results, the better (minimum) fuel costs offered by AOA algorithm is 799.1543 \$/hr which is better than that determined by the other compared algorithms. Furthermore, Figure 1 shows the voltage profile of the AOA which guarantees that the magnitudes of all voltages for all buses are within acceptable limits. Figure 2 depicts the convergence characteristics of minimizing the fuel cost (more than 200 iterations) produced by the standard AOA and other algorithms compared. It is observed that from this figure the AOA yields better convergence characteristics than other compared algorithms.

4.1.2. Case2: Minimization of active power losses

For this case, the minimization of the real power loss is considered here as a single objective function. The best simulation results yielded based on the AOA are presented in Table 2 together with the obtained results of the other compared techniques, where AOA yielded power losses value of 2.980374 MW compared to the results of 4.417859, 3.414704, 3.774816 and 3.8095 MW achieved by FSA, SSA, PSO and DA respectively. As in case 1, the voltages profile for all buses are within their boundaries as shown in Figure 3. The minimizing real power loss convergence characteristics obtained by AOA and other compared techniques is illustrated in Figure 4, it is concluded that the AOA's convergence characteristics of minimizing real power loss outperform with the other algorithms that were compared.

Table 1. Optimal control variables for IEEE30-bus test system for minimizing fuel cost

	FSA	SSA	PSO	DA	AOA
P_{G2} (MW)	46.28349	80	48.87814	48.93911	48.25165
P_{G5} (MW)	21.34807	15	21.47237	21.32534	21.40734
P_{G8} (MW)	23.26794	35	21.68903	21.33967	21.2471
P_{G11} (MW)	14.56352	30	10	10	12.40777
P_{G13} (MW)	16.68156	24.4285	12	12	11.11124
V_1 (pu)	1.088163	0.95	1.1	1.1	1.099999
V_2 (pu)	1.078415	1.1	1.086457	1.075001	1.086588
V_5 (pu)	1.035299	1.070375	1.058621	1.034858	1.059408
V_8 (pu)	1.049452	1.073196	1.066039	1.048098	1.068567
V_{11} (pu)	1.083961	1.1	1.08413	1.1	1.099741
V_{13} (pu)	1.094221	1.042241	1.1	1.1	1.099967
T_{11} (6-9)	1.029402	0.9	0.9	0.995808	0.997018
T_{12} (6-10)	1.078941	0.981035	1.1	1.008401	0.987031
T_{15} (4-12)	1.062136	1.08085	1.030829	1.010048	1.005459
T_{36} (2827)	0.968044	0.9	0.980481	0.96689	0.981402
Q_{10} (MVR)	0.335860	0	0	2.614276	2.898496
Q_{12} (MVR)	0.335860	0.378800	4.999604	2.327550	2.511993
Q_{15} (MVR)	0.335860	0.098791	5	1.707832	4.557046
Q_{17} (MVR)	0.335860	5	5	1.936540	4.807264
Q_{20} (MVR)	0.335860	0	5	5	4.578255
Q_{21} (MVR)	0.335860	0.205703	5	4.697618	4.954453
Q_{23} (MVR)	0.335860	2.563488	0	2.858147	2.354573
Q_{24} (MVR)	0.335860	3.784069	5	2.801551	4.362404
Q_{29} (MVR)	0.335860	5	3.426363	5	3.406998
Fuel Cost (\$/h)	802.7119	817.6356	799.5118	800.1055	799.1543
Power Losses (MW)	8.711178	25.18706	8.804382	9.023054	8.663665
Voltage Deviations(pu)	0.506489	1.438624	1.472048	1.283183	1.583447

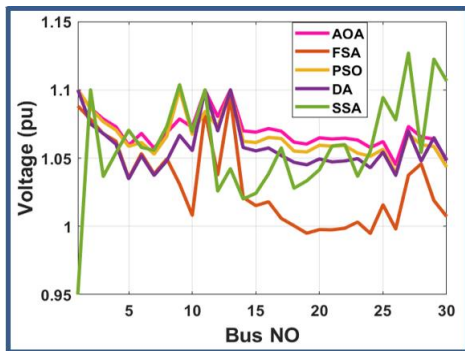


Figure 1. The voltage profile of the AOA and other compared algorithms for case 1

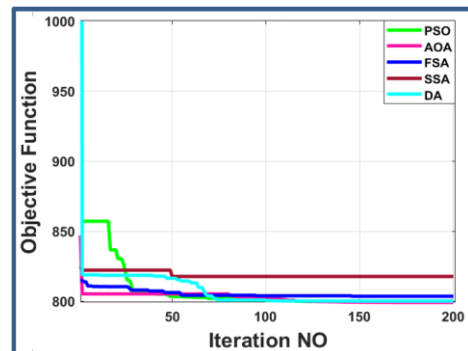


Figure 2. The convergence characteristics of AOA and other compared algorithms for case 1

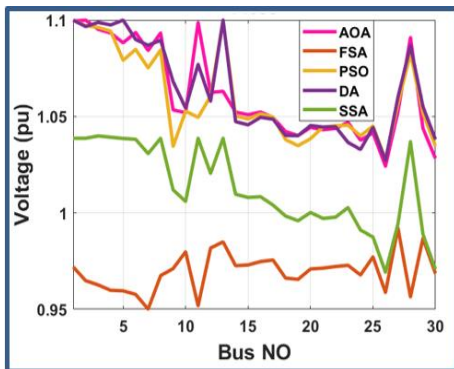


Figure 3. The voltage profile of the AOA and other AOA compared algorithms for case 2

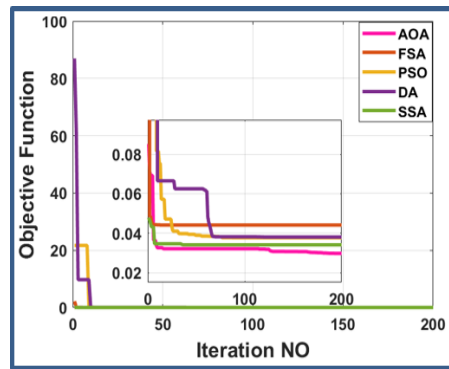


Figure 4. The convergence characteristics of AOA and other compared algorithms for case 2

Table 2. Optimal control variables for IEEE30-bus test system for minimizing real power loss

	FSA	SSA	PSO	DA	AOA
P_{G2} (MW)	73.00357	80	80	76.21227	79.9728
P_{G5} (MW)	43.56395	50	50	50	49.99981
P_{G8} (MW)	34.90729	35	35	26.88553	34.7412
P_{G11} (MW)	30	30	10	21.95056	29.92457
P_{G13} (MW)	37.92178	40	40	40	39.91039
V_1 (pu)	0.97198	1.038716	1.1	1.1	1.099507
V_2 (pu)	0.964838	1.038704	1.097106	1.096669	1.099963
V_5 (pu)	0.959585	1.038594	1.079159	1.1	1.088233
V_8 (pu)	0.967453	1.038695	1.084461	1.089537	1.093303
V_{11} (pu)	0.951831	1.038707	1.049517	1.077027	1.098702
V_{13} (pu)	0.984971	1.038704	1.1	1.1	1.063046
T_{11} (6-9)	0.979798	1.038544	1.1	1.002769	1.079032
T_{12} (6-10)	0.900415	1.038584	0.9	1.024754	1.010058
T_{15} (4-12)	0.984489	1.038668	1.1	1.1	1.019467
T_{36} (28-27)	0.947636	1.038656	1.015115	1.007676	1.021381
Q_{10} (MVAR)	5	5	5	5	4.952362
Q_{12} (MVAR)	5	5	5	1.823587	4.656925
Q_{15} (MVAR)	5	5	5	5	4.600773
Q_{17} (MVAR)	5	5	5	1.878693	4.872392
Q_{20} (MVAR)	5	5	0	5	4.133455
Q_{21} (MVAR)	5	5	5	4.996018	4.086306
Q_{23} (MVAR)	5	5	3.740602	0	4.792458
Q_{24} (MVAR)	5	5	5	0	3.561832
Q_{29} (MVAR)	5	5	5	5	3.707280
Fuel Cost (\$/h)	923.4265	968.4138	938.6007	936.42	966.5503
Power Losses (MW)	4.417859	3.414704	3.774816	3.8095	2.980374
Voltage Deviations(pu)	0.714313	0.365503	1.283244	1.34055	1.31844

4.1.3. Case3: Minimization of total voltage deviation

The proposed AOA is employed in this case, for minimizing the total Voltage deviation discussed in section 2 as single objective function. The Table 3 shows the optimal variables resulting by AOA alongside with the other compared algorithms, where the best and minimum voltage deviation value is 0.120906 pu which observed with AOA compared to 0.138711 pu, 0.306075 pu, 0.181846 pu and 0.291642 pu with FSA, SSA, PSO and DA respectively. According to Figure 5, it is seen that the AOA also offer the best voltage profile than the other compared algorithms. Also, Figure 6 proven that the convergence characteristic obtained by the AOA outperforms those by the other compared algorithm.

Table 3. Optimal control variables for IEEE 30-bus test system for minimizing voltage deviation

	FSA	SSA	PSO	DA	AOA
P_{G2} (MW)	46.20759	79.72873	80	43.42174	9.7903
P_{G5} (MW)	30.90417	50	15.79909	29.08509	45.8976
P_{G8} (MW)	23.94749	35	34.98085	31.68695	21.7849
P_{G11} (MW)	20.39471	30	13.34155	25.99727	28.3488
P_{G13} (MW)	25.34568	40	12.28699	24.50418	18.0528
V_1 (pu)	1.015291	1.023154	1.046164	1.088389	1.012223
V_2 (pu)	1.005648	1.023334	1.02455	1.04562	0.997005
V_5 (pu)	1.019072	1.023358	1.021993	1.009017	1.019623
V_8 (pu)	1.007426	1.023358	0.99251	0.990572	1.007383
V_{11} (pu)	1.023104	1.023177	1.043296	1.085419	1.039686
V_{13} (pu)	0.992756	1.023193	1.061513	1.02474	1.036563
T_{11} (6-9)	0.939334	1.023104	0.902244	0.950507	0.991073
T_{12} (6-10)	1.01692	1.023379	1.1	0.943128	0.934161
T_{15} (4-12)	0.976926	1.023246	1.1	1.1	1.008232
T_{36} (28-27)	0.963545	1.023257	0.938548	0.96876	0.956226
Q_{10} (MVAR)	5	5	4.992005	4.522767	3.992631
Q_{12} (MVAR)	5	5	5	2.504991	1.905802
Q_{15} (MVAR)	4.849158	5	5	5	4.122284
Q_{17} (MVAR)	5	5	0.347174	2.894850	2.425013
Q_{20} (MVAR)	4.910406	5	5	2.732917	4.994577
Q_{21} (MVAR)	5	5	0	5	4.847301
Q_{23} (MVAR)	5	5	5	2.416678	4.212442
Q_{24} (MVAR)	4.922147	5	5	0.582945	4.3825691
Q_{29} (MVAR)	5	5	0	2.658813	1.3320663
Fuel Cost (\$/h).	822.525	968.0146	832.2631	828.1918	860.1368
Power Losses (MW).	7.934595	3.492302	8.511614	7.666995	10.44553
Voltage Deviations(pu)	0.138711	0.306075	0.181846	0.291642	0.120906

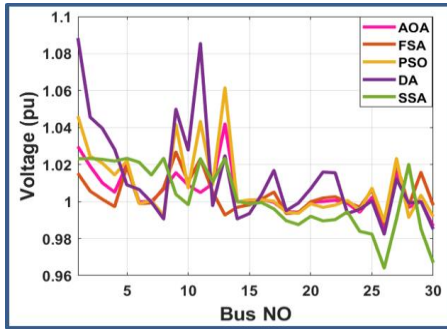


Figure 5. The voltage profile of the AOA and other compared algorithms for case3

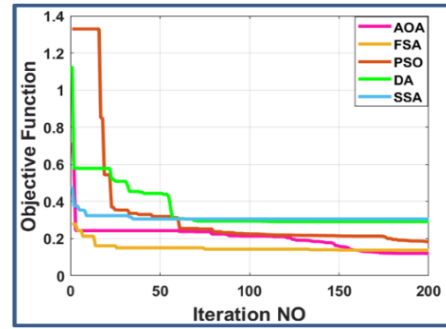


Figure 6. The convergence characteristics of AOA and other compared algorithms for case3

4.1.4. Case4: Minimization of multi objective function without emission

For optimizing more than single objective function, simultaneously, the multi-objective function using weighting factors as discussed in section 2 is proposed here for obtaining the maximum benefits of the proposed test system. Table 4 shows how the AOA and other compared algorithms solved the multi-objective OPF problem without considering emission in the IEEE-30 bus system. These findings suggest that using AOA to solve the multi-objective OF problem is more effective than using other compared algorithms. Where, the total objective function with the value of 836.3664 \$/hr is better than all other algorithms with the results 847.2615 \$/hr, 926.823 \$/hr, 844.1233\$/hr and 845.088 \$/hr achieved by FSA, SSA, PSO and DA respectively without violating the consider constraints. As in previous cases, the voltage profiles of all buses are within the specified limits, as shown in Figure 7, for all compared algorithms. Furthermore, as shown in Figure 8, the AOA still has fast and smooth convergence characteristics when compared to other algorithms.

Table 4. Optimal control variables for IEEE30-bus test system for minimizing multi-objective function without emission

	FSA	SSA	PSO	DA	AOA
P_{G2} (MW)	55.78434	46.83946	48.60174	47.89617	49.16384
P_{G5} (MW)	24.03921	25.81327	22.56217	23.61245	22.79406
P_{G8} (MW)	19.01405	35	23.80653	19.69738	26.21244
P_{G11} (MW)	15.74422	27.06992	13.42591	20.53271	15.30012
P_{G13} (MW)	24.79774	35.95446	12	12.0331	11.4444
V_1 (pu)	1.024729	1.037957	1.1	1.043497	1.052391
V_2 (pu)	1.014104	1.012106	1.060285	1.028974	1.033897
V_5 (pu)	1.002711	0.962564	1.008819	1.036575	1.004587
V_8 (pu)	1.0187	1.018687	1.000206	0.999347	1.000761
V_{11} (pu)	1.03556	0.96675	1.053441	1.029754	1.017336
V_{13} (pu)	1.010232	1.050623	0.991688	1.016487	1.036494
T_{11} (6-9)	1.00081	0.997347	0.928706	0.925325	0.978556
T_{12} (6-10)	1.030657	0.957128	1.098984	1.050108	0.959816
T_{15} (4-12)	0.99651	1.030978	0.944668	0.945414	1.041585
T_{36} (28-27)	0.989278	0.907406	0.949064	0.953255	0.957001
Q_{10} (MVAR)	5	5	4.945975	4.941679	3.181699
Q_{12} (MVAR)	5	5	0	3.204882	3.6623086
Q_{15} (MVAR)	5	5	4.708812	1.703036	4.6046683
Q_{17} (MVAR)	5	5	0	1.821205	0.2866086
Q_{20} (MVAR)	5	5	4.999873	5	4.6719239
Q_{21} (MVAR)	5	5	5	1.237059	4.8645306
Q_{23} (MVAR)	5	5	0	0.703911	4.6938668
Q_{24} (MVAR)	5	5	5	2.438956	4.2484880
Q_{29} (MVAR)	5	5	0	2.399590	1.6325226
Q_{29} (MVAR)	5	5	0	2.399590	1.6325226
Objective Functions	847.2615	926.823	844.1233	845.088	836.3664
Fuel Cost (\$/h)	812.9506	843.7939	804.9762	807.5542	803.6294
Power Losses (MW)	8.636995	6.688798	9.842343	9.652608	8.871927
Voltage Deviations(pu)	0.170159	0.428451	0.194624	0.182286	0.149931

4.1.5. Case5: Minimization of multi objective function with emission

The best results of solving a multi-objective OPF problem with considering emission for IEEE 30-bus testing system attained by the AOA algorithm is shown in Table 5. From this table, it can be observed

that the AOA outperforms other compared algorithms with it. As well as the AOA provides a best value of 865.9021 \$/hr towards 878.1909 \$/hr, 902.4330 \$/hr, 877.0695 \$/hr, and 888.3333 \$/hr with the FSA, SSA, PSO and DA respectively. The voltages profile of all buses in this case is given in Figure 9, it is recognized that all voltages within specified limits for all compared algorithms. Moreover, the convergence characteristics for this case obtained by AOA and other algorithms is shown in Figure 10, where AOA convergence characteristic has fast and speed convergence, so it outperforms all other algorithms.

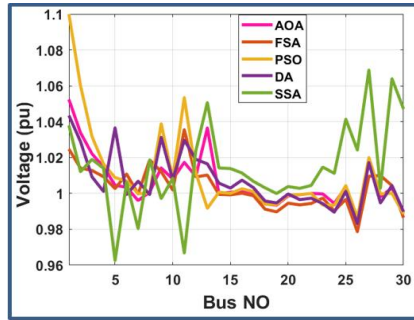


Figure 7. The voltage profile of the AOA and other compared algorithms for case4

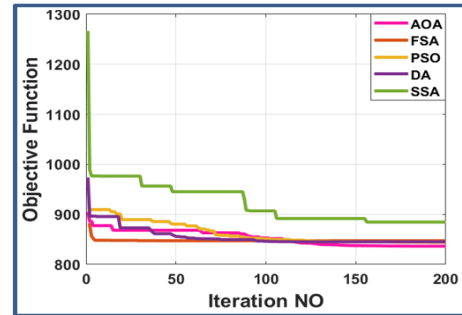


Figure 8. The convergence characteristics of AOA and other compared algorithms for case4

Table 5. Optimal control variables for IEEE30-bus test system for minimizing multi-objective function with emission

	<i>FSA</i>	<i>SSA</i>	<i>PSO</i>	<i>DA</i>	<i>AOA</i>
P_{G2} (MW)	61.9489	27.3040	48.2291	49.3112	52.22681
P_{G5} (MW)	23.1307	28.2910	22.1052	15.0505	22.71533
P_{G8} (MW)	21.6630	31.6452	35	25.9489	21.38361
P_{G11} (MW)	21.2544	26.3380	10	19.9303	14.97433
P_{G13} (MW)	21.3232	21.9211	12	15.1212	12.98854
V_1 (pu)	1.0311	1.0762	1.1000	1.0391	1.0445
V_2 (pu)	1.0233	1.0307	1.0560	1.0263	1.0267
V_5 (pu)	0.9937	0.9553	1.0071	0.9940	1.0084
V_8 (pu)	1.0058	0.9785	0.9961	1.0192	0.9999
V_{11} (pu)	1.0026	1.0047	1.1000	1.0378	1.0328
V_{13} (pu)	1.0248	1.0198	0.9879	1.1000	1.0077
T_{11} (6-9)	0.9562	0.9501	0.9497	1.0116	1.0177
T_{12} (6-10)	1.0206	0.9501	1.1000	1.0387	0.9255
T_{15} (4-12)	1.0051	0.9501	0.9645	1.0472	0.9851
T_{36} (28-27)	0.9879	0.9053	0.9626	0.9639	0.9648
Q_{10} (MVAR)	5	0.5307	5	0	3.8646
Q_{12} (MVAR)	5	4.0843	5	2.39735	2.8986
Q_{15} (MVAR)	5	4.7024	3.9236	1.89627	4.9887
Q_{17} (MVAR)	5	4.6202	0	2.10729	0.5656
Q_{20} (MVAR)	5	2.8588	5	3.97871	4.9662
Q_{21} (MVAR)	5	3.7336	0.01161	1.34798	4.8238
Q_{23} (MVAR)	5	3.00002	5	1.64823	4.9771
Q_{24} (MVAR)	5	1.05593	5	1.92027	4.3078
Q_{29} (MVAR)	5	0.53077	1.400453	5	2.6792
Objective Function	878.1909	902.4330	877.0695	888.3333	865.9021
Fuel Cost (\$/h)	816.1303	829.7243	807.4802	809.0444	804.0073
Power Losses (MW)	7.8104	8.7264	9.418377	809.0444	9.210662
Voltage Deviations (pu)	0.1578	0.2474	0.195761	0.2906	0.120500

4.1.6. Case6: Optimal allocation for renewable energy sources for minimizing fuel cost

Where the integration of various renewable sources in the electrical power system increases the degree of sophistication of the OPF problem as discussed in section 1, therefore, to show and confirm the efficacy of the AOA proposed and implemented in this case to find the optimal allocation of renewable energy sources and applied on the IEEE-30 bus testing system for minimizing the fuel costs. Table 6 illustrates the best AOA results as well as those obtained by other algorithms. According to the simulated results, AOA algorithm introduces better (minimum) fuel cost with the optimal location at bus 25 with 766.0242 \$/hr which is better than that determined at bus 30 by the other compared algorithms with values of 782.489 \$/hr, 917.122 \$/hr, and 857.0542 \$/hr with the FSA, SSA and PSO respectively. Furthermore, Figure 11 show the voltage profile of the AOA that guarantees that all voltage magnitudes for all buses are

within acceptable limits. The convergence characteristics of minimizing the fuel cost yielded by AOA and other compared algorithms are shown in Figure 12. According to this figure, the AOA produces better convergence characteristics than the other compared algorithms.

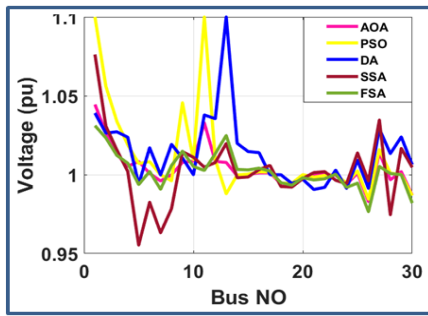


Figure 9. The voltage profile of the AOA and other compared algorithms for case 5

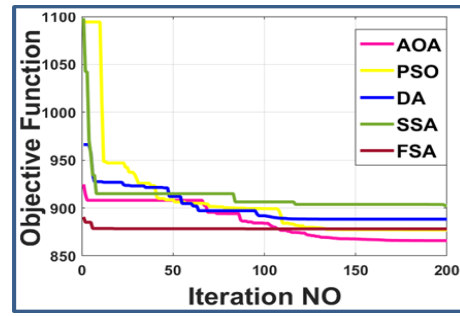


Figure 10. The convergence characteristics of AOA and other compared algorithms for case 5

Table 6. Optimal RES allocation for IEEE 30-bus testing system for minimizing the fuel costs

	DG Location	DG Size		F_{cost}	P_{loss}	VD
		MW	MVA _r			
Base Case	-	-	-	11214.41	5.82226	1.14965
FSA	30	0.456018	0.2212981	782.489	6.35690	0.86232
SSA	30	0.253229	0.1579159	917.122	4.83847	0.78772
PSO	30	0.194454	0.1643651	857.0542	4.83432	0.76938
AOA	25	0.484643	0.2443312	776.0242	5.09091	0.63354

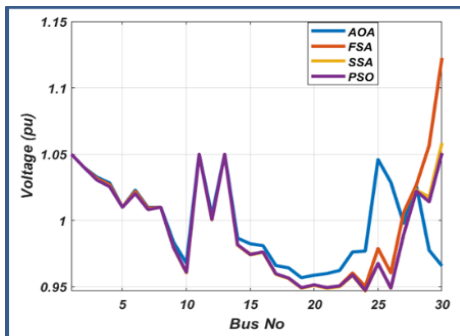


Figure 11. The voltage profile of the AOA and other compared algorithms for case 6

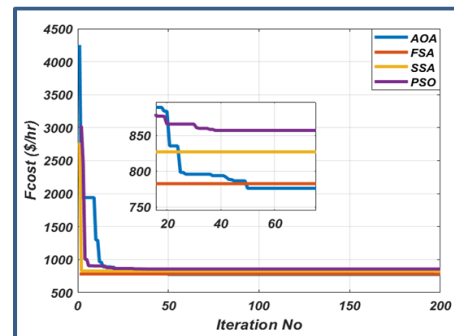


Figure 12. The convergence characteristics of AOA and other compared algorithms for case 6

4.1.7. Minimization of the fuel cost with the penetration of RES

For the present case, to prove the efficiency of the proposed AOA algorithm, it compared also with different recent algorithms to minimize and solve the OPF problem with a single objective function represented in the reduction of fuel cost only and testing them on a modified IEEE 30-bus system that included RES integrated with optimal allocation as present in case 6. Table 7 illustrates the results for this case, where AOA yielded the best (minimum) fuel cost of 635.8983 \$/hr, compared with 646.264547 \$/hr, 688.92437 \$/hr, 639.26731 \$/hr, 637.9108 \$/hr, achieved by FSA, SSA, PSO and DA respectively. In addition, comparing with the first case the superiority of the proposed AOA algorithm is proven, where in case 1, AOA introduce minimization of fuel cost with value of 799.1543 \$/hr which is higher than that determined by introduce proposed AOA with the integration of renewable energy source which adding complexity of the optimal power flow problem and achieve fuel cost minimization with value of 635.8983 \$/hr which is less than that determined in case1. Figure 13 illustrates the voltage profiles for all buses that are within their boundaries. also, Figure 14 depicts the convergence characteristics of fuel cost by AOA and other compared techniques, demonstrating that the AOA's convergence characteristics outperform those of the other algorithms compared with it.

Table 7. Optimal control variables for modified IEEE30-bus test system for minimizing fuel cost

	FSA	SSA	PSO	DA	AOA
P_{G1} (MW)	134.328203	87.663917	153.90287	146.5862	157.6299
P_{G2} (MW)	50.1318584	64.489854	43.164128	41.74496	42.98818
P_{G5} (MW)	16.6277722	15.333046	15	19.46930	19.78803
P_{G8} (MW)	11.8628598	28.127361	10	10.91869	7.860474
P_{G11} (MW)	16.7113467	22.939775	10	12.48998	7.891434
P_{G13} (MW)	13.7670858	24.179165	12	12	7.627846
V_1 (pu)	1.07213437	0.9875585	1.1	1.1	1.098665
V_2 (pu)	1.06370895	0.9714789	1.0891724	1.091534	1.084298
V_5 (pu)	1.07218239	0.9669598	1.0634733	1.075556	1.056581
V_8 (pu)	1.04296082	0.9543305	1.0744262	1.073636	1.065559
V_{11} (pu)	1.07222602	0.9778671	1.1	1.016967	1.048832
V_{13} (pu)	1.04296081	0.9528972	0.95	1.055537	1.047008
T_{11} (6-9)	1.03729456	0.9	1.1	1.026075	0.977883
T_{12} (6-10)	1.07213628	0.9184583	1.1	1.022914	1.030724
T_{15} (4-12)	1.07214024	0.9686594	1.1	1.022754	0.998454
T_{36} (28-27)	1.07226459	0.9106857	1.1	1.1	1.077131
Q_{10} (MVAR)	2.67969912	0.4441304	0	3.149833	2.603767
Q_{12} (MVAR)	2.67969912	1.4258255	5	2.155722	1.15499
Q_{15} (MVAR)	2.67969912	3.0397021	5	3.474743	1.84191
Q_{17} (MVAR)	2.67969912	0.8107773	0	3.012264	2.213119
Q_{20} (MVAR)	2.67969912	4.4382199	5	0	3.070424
Q_{21} (MVAR)	2.67969912	0.5554283	5	0	3.407764
Q_{23} (MVAR)	2.67969912	0.4320592	0	1.879185	2.980572
Q_{24} (MVAR)	2.67969912	1.0959013	0	0.982048	2.07048
Q_{29} (MVAR)	2.67969912	1.2720052	5	1.774889	1.299162
Fuel Cost (\$/h)	646.264547	688.92437	639.26731	637.9108	635.8983
Power Losses (MW)	8.49342960	7.7974323	9.1313042	8.273496	8.850231
Voltage Deviations(pu)	0.64801769	0.9041885	0.9617804	0.875053	1.11413

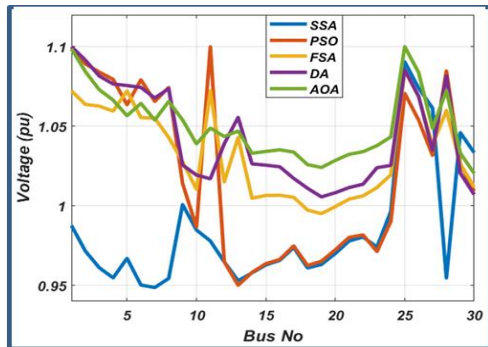


Figure 13. The voltage profile of the AOA and other compared algorithms for case 7

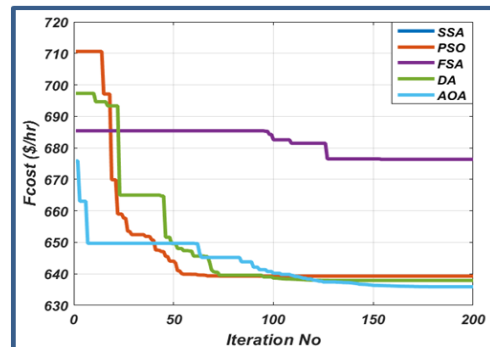


Figure 14. The convergence characteristics of AOA and other compared algorithms for case 7

5. CONCLUSION

In order to solve the OPF problem considering the fuel cost, power loss, voltage profile improvement and emissions, a new metaheuristic algorithm has been investigated in this paper. The efficacy and supremacy of AOA have been evaluated based on standards for solving and optimizing the single-objective and multi-objective function of OPF problems and modified testing system of IEEE-30 bus with the presence of RES to prove its efficiency in finding the optimal allocation with minimization of fuel cost. According to the results, the AOA provided a better mitigation of the objective functions in all cases than other recently compared algorithms. The comparison results clearly show that the AOA outperformed these recent algorithms regardless of the type of objective function, indicating the AOA's ability to solve other real-life applications.

REFERENCES




- [1] M. A. M. Shaheen, H. M. Hasanien, S. F. Mekhamer and H. E. A. Talaat, "Optimal Power Flow of Power Networks with Penetration of Renewable Energy Sources By Harris hawks Optimization Method," *2nd International Conference on Smart Power & Internet Energy Systems (SPIES)*, 2020, pp. 537-542, doi: 10.1109/SPIES48661.2020.9242932.
- [2] P. P. Biswas, P. N. Suganthan, R. Mallipeddi, and G. A. J. Amaratunga, "Multi-objective optimal power flow solutions using a constraint handling technique of evolutionary algorithms," *Soft Computing*, vol. 24, no. 4, pp. 2999-3023, 2020.
- [3] Z. Ullah et al., "A Mini-review: Conventional and Metaheuristic Optimization Methods for the Solution of Optimal Power Flow

- (OPF) Problem,” *International Conference on Advanced Information Networking and Applications*, 2020, vol. 1151 AISC, pp. 308-319, doi: 10.1007/978-3-030-44041-1_29.
- [4] C. Shilaja, and T. Arunprasath, “Optimal power flow using moth swarm algorithm with gravitational search algorithm considering wind power,” *Future Generation Computer Systems*, vol. 98, pp. 708-715, doi: 10.1016/j.future.2018.12.046.
- [5] E. E. Elattar and S. K. Elsayed, “Modified JAYA algorithm for optimal power flow incorporating renewable energy sources considering the cost, emission, power loss and voltage profile improvement,” *Energy*, vol. 178, pp. 598-609, 2019, doi: 10.1016/j.energy.2019.04.159.
- [6] G. Chen, J. Qian, Z. Zhang, and Z. Sun, “Multi-objective Improved Bat Algorithm for Optimizing Fuel Cost, Emission and Active Power Loss in Power System,” *IAENG International Journal of Computer Science*, vol. 46, no. 1, pp. 1-16, 2020.
- [7] M. A. M. Shaheen, H. M. Hasanien, S. F. Mekhamer and H. E. A. Talaat, “Optimal Power Flow of Power Systems Including Distributed Generation Units Using Sunflower Optimization Algorithm,” *IEEE Access*, vol. 7, pp. 109289-109300, 2019, doi: 10.1109/ACCESS.2019.2933489.
- [8] M. K. Ahmed, M. H. Osman, A. A. Shehata and N. V. Korovkin, “A Solution of Optimal Power Flow Problem in Power System Based on Multi Objective Particle Swarm Algorithm,” *IEEE Conference of Russian Young Researchers in Electrical and Electronic Engineering (ElConRus)*, 2021, pp. 1349-1353, doi: 10.1109/ElConRus51938.2021.9396117.
- [9] M. Ebeed, S. Kamel, and F. Jurado, “Optimal power flow using recent optimization techniques,” *Classical and Recent Aspects of Power System Optimization*, pp. 157-183, 2018, doi: 10.1016/B978-0-12-812441-3.00007-0.
- [10] H. Buch and I. N. Trivedi, “On the efficiency of metaheuristics for solving the optimal power flow,” *Neural Computing and Applications*, vol. 31, no. 9, pp. 1-9, 2018, doi: 10.1007/s00521-018-3382-8.
- [11] B. Stott and E. Hobson, “Power System Security Control Calculations Using Linear Programming, Part I,” *IEEE Transactions on Power Apparatus and Systems*, vol. PAS-97, no. 5, pp. 1713-1720, 1978, doi: 10.1109/TPAS.1978.354664.
- [12] A. M. Sasson, “Decomposition Techniques Applied to the Nonlinear Programming Load-Flow Method,” *IEEE Transactions on Power Apparatus and Systems*, vol. PAS-89, no. 1, pp. 78-82, 1970, doi: 10.1109/TPAS.1970.292671.
- [13] G. C. Contaxis, C. Delkis and G. Korres, “Decoupled Optimal Load Flow Using Linear or Quadratic Programming,” *IEEE Transactions on Power Systems*, vol. 1, no. 2, pp. 1-7, 1986, doi: 10.1109/TPWRS.1986.4334888.
- [14] S.-D. Chen, and J.-F. Chen, “A new algorithm based on the Newton-Raphson approach for realtime emission dispatch,” *Electric Power Systems Research*, vol. 40, no. 2, pp. 137-141, 1997, doi: 10.1016/S0378-7796(96)01145-5.
- [15] J. A. Momoh, R. F. Austin, R. Adapa and E. C. Ogbuobiri, “Application of interior point method to economic dispatch,” *Proceedings IEEE International Conference on Systems, Man, and Cybernetics*, 1992, pp. 1096-1101 vol. 2, doi: 10.1109/ICSMC.1992.271643.
- [16] H. Jadhav and P. Bamane, “Temperature dependent optimal power flow using g-best guided artificial bee colony algorithm,” *International Journal of Electrical Power & Energy Systems*, vol. 77, pp. 77-90, 2016, doi: 10.1016/j.ijepes.2015.11.026.
- [17] S.S. Reddy, and C.S. Rathnam, “Optimal power flow using glowworm swarm optimization,” *International Journal of Electrical Power & Energy Systems*, vol. 80, pp. 128-139, 2016, doi: 10.1016/j.ijepes.2016.01.036.
- [18] Y. Tan *et al.*, “Improved group search optimization method for optimal power flow problem considering valve-point loading effects,” *Neurocomputing*, vol. 148, pp. 229-239, 2015, doi:10.1016/j.neucom.2013.09.065.
- [19] A. Mukherjee, and V. Mukherjee, “Solution of optimal power flow with FACTS devices using a novel oppositional krill herd algorithm,” *International Journal of Electrical Power & Energy Systems*, vol. 78, pp. 700-714, 2016, doi: 10.1016/J.IJEPES.2015.12.001.
- [20] K. Ayan, U. Kilic and B. Baraklı, “Chaotic artificial bee colony algorithm based solution of security and transient stability constrained optimal power flow,” *International Journal of Electrical Power & Energy Systems*, vol. 64, pp. 136-147, doi: 10.1016/J.IJEPES.2014.07.018.
- [21] A. Mukherjee and V. Mukherjee, “Solution of optimal power flow using chaotic krill herd algorithm,” *Chaos, Solitons & Fractals*, vol. 78, pp. 10-21, 2015, doi: 10.1016/J.CHAOS.2015.06.020.
- [22] A. A. A. Mohamed, Y. S. Mohamed, A. A. El-Gaafary, and A. M. Hemeida, “Optimal power flow using moth swarm algorithm,” *Electric Power Systems Research*, vol. 142, pp. 190-206, 2017, doi: 10.1016/J.EPSR.2016.09.025.
- [23] N. Sinsuphan, U. Leeton, and T. Kulworawanichpong, “Optimal power flow solution using improved harmony search method,” *Applied Soft Computing*, vol. 13, no. 5, pp. 2364-2374, 2013, doi:10.1016/j.asoc.2013.01.024.
- [24] S. Duman, “Symbiotic organisms search algorithm for optimal power flow problem based on valve-point effect and prohibited zones,” *Neural Computing and Applications*, vol. 28, pp. 1-15, 2017, doi: 10.1007/s00521-016-2265-0.
- [25] M. R. Adaryani, and A. Karami, “Artificial bee colony algorithm for solving multi-objective optimal power flow problem,” *International Journal of Electrical Power & Energy Systems*, vol. 53, pp. 219-230, 2013, doi: 10.1016/J.IJEPES.2013.04.021.
- [26] M. Ghasemi, S. Ghavidel, M. Gitizadeh, and E. Akbari, “An improved teaching-learning-based optimization algorithm using Levy mutation strategy for non-smooth optimal power flow,” *International Journal of Electrical Power & Energy Systems*, vol. 65, pp. 375-384, 2015, doi: 10.1016/J.IJEPES.2014.10.027.
- [27] B. Mandal, and P. K. Roy, “Multi-objective optimal power flow using quasi-oppositional teaching learning based optimization,” *Applied Soft Computing*, vol. 21, pp. 590-606, doi: 10.1016/j.asoc.2014.04.010.
- [28] P. Somasundaram, K. Kuppusamy and R. K. Devi, “Evolutionary programming based security constrained optimal power flow,” *Electric Power Systems Research*, vol. 72, no. 2, pp. 137-145, 2004, doi: 10.1016/J.EPSR.2004.02.006.
- [29] S. S. Reddy, P. Bijwe, and A. Abhyankar, “Faster evolutionary algorithm based optimal power flow using incremental variables,” *International Journal of Electrical Power & Energy Systems*, vol. 54, pp. 198-210, 2014, doi: 10.1016/J.IJEPES.2013.07.019.
- [30] X. Yuan *et al.*, “Multi-objective optimal power flow based on improved strength Pareto evolutionary algorithm,” *Energy*, vol. 122, pp. 70-82, 2017, doi: 10.1016/J.ENERGY.2017.01.071.
- [31] H. Pulluri, R. Naresh, and V. Sharma, “An enhanced self-adaptive differential evolution based solution methodology for multiobjective optimal power flow,” *Applied Soft Computing*, vol. 54, pp. 229-245, 2017, doi: 10.1016/j.asoc.2017.01.030.
- [32] S. S. Reddy, and P. Bijwe, “Differential evolution-based efficient multi-objective optimal power flow,” *Neural Computing and Applications*, pp. 1-14, 2017, doi: 10.1007/s00521-017-3009-5.
- [33] A. Chaib, H. Bouchekara, R. Mehasni, and M. Abido, “Optimal power flow with emission and nonsmooth cost functions using backtracking search optimization algorithm,” *International Journal of Electrical Power & Energy Systems*, vol. 81, pp. 64-77, 2016, doi: 10.1016/J.IJEPES.2016.02.004.
- [34] H. R.E. H. Bouchekara, A. E. Chaib, M. A. Abido, and R. A. El-Sehiemy, “Optimal power flow using an improved colliding bodies optimization algorithm,” *Applied Soft Computing*, vol. 42, pp. 119-131, doi: 10.1016/j.asoc.2016.01.041.
- [35] A. Gacem and D. Benatous, “Hybrid genetic algorithm and particle swarm for optimal power flow with non-smooth fuel cost functions,” *International Journal of System Assurance Engineering and Management*, vol. 8, pp. 146-153, 2014, doi:10.1007/S13198-014-0312-8.
- [36] M. Joorabian, and E. Afzalan, “Optimal power flow under both normal and contingent operation conditions using the hybrid fuzzy particle swarm optimisation and Nelder-Mead algorithm (HFPSO-NM),” *Applied Soft Computing*, vol. 14, pp. 623-633, 2014, doi: 10.1016/j.asoc.2013.09.015.




- [37] R. P. Singh, V. Mukherjee, and S. Ghoshal, "Particle swarm optimization with an aging leader and challengers algorithm for the solution of optimal power flow problem," *Applied Soft Computing*, vol. 40, pp. 161-177, 2016, doi:10.1016/j.asoc.2015.11.027.
- [38] T. T. Nguyen, "Neural network optimal-power-flow," *Fourth International Conference on Advances in Power System Control, Operation and Management, APSCOM-97. (Conf. Publ. No. 450)*, 1997, pp. 266-271 vol.1, doi: 10.1049/cp:19971842.
- [39] B. Venkatesh, "Online ANN memory model-based method for unified OPF and voltage stability margin maximization," *Electric Power Components and Systems*, vol. 31, no. 5, pp. 453-465, 2010, doi: 10.1080/15325000390127002.
- [40] V. C. Ramesh, and X. Li, "Optimal power flow with fuzzy emissions constraints," *Electric Machines & Power Systems*, vol. 25, no. 8, pp. 897-906, 1997, doi: 10.1080/07313569708955784.
- [41] B. Baydar, M. C. Taplamacıoğlu and H. Gözde, "Investigation of the effect of renewable energy sources on static voltage stability with dynamic optimal power flow solution in power systems," *6th International Istanbul Smart Grids and Cities Congress and Fair (ICSG)*, 2018, pp. 203-207, doi: 10.1109/SGCF.2018.8408973.
- [42] A. A. E. Ela, R. A. El-Sehiemy, M. T. Mouwafi and D. A. Salman, "Multiobjective Fruit Fly Optimization Algorithm for OPF Solution in Power System," *Twentieth International Middle East Power Systems Conference (MEPCON)*, 2018, pp. 254-259, doi: 10.1109/MEPCON.2018.8635232.
- [43] M. Abbasi, E. Abbasi, and B. M. Ivatloo, "Single and multi-objective optimal power flow using a new differential-based harmony search algorithm," *Journal of Ambient Intelligence and Humanized Computing*, vol. 12, no. 1, pp. 851-871, 2021 doi: 10.1007/s12652-020-02089-6.
- [44] G. Chen, J. Qian, Z. Zhang, and S. Li, "Application of modified pigeon-inspired optimization algorithm and constraint-objective sorting rule on multi-objective optimal power flow problem," *Applied Soft Computing Journal*, vol. 92, 2020, doi: 10.1016/j.asoc.2020.106321.
- [45] G. Chen, J. Qian, Z. Zhang and Z. Sun, "Multi-Objective Optimal Power Flow Based on Hybrid Firefly-Bat Algorithm and Constraints-Prior Object-Fuzzy Sorting Strategy," *IEEE Access*, vol. 7, pp. 139726-139745, 2019, doi: 10.1109/ACCESS.2019.2943480.
- [46] I. B. M. Taha and E. E. Elattar, "Optimal reactive power resources sizing for power system operations enhancement based on improved grey wolf optimizer," *IET Generation, Transmission & Distribution*, vol. 12, no. 14, pp. 3421-3434, 2018, doi: 10.1049/iet-gtd.2018.0053.
- [47] O. Alsac and B. Stott, "Optimal Load Flow with Steady-State Security," *IEEE Transactions on Power Apparatus and Systems*, vol. PAS-93, no. 3, pp. 745-751, 1974, doi: 10.1109/TPAS.1974.293972.
- [48] Washington university website, last accessed 1 november 2018. [Online] Available: www.ee.washington.edu/research/pstca/.
- [49] M. A. Abido, "Multiobjective particle swarm optimization for optimal power flow problem," *Handbook of swarm intelligence*, Springer, Berlin, Heidelberg, pp. 241-268, 2011, doi: 10.1109/MEPCON.2008.4562380.
- [50] H. Ouafa, S. Linda and B. Tarek, "Multi-objective optimal power flow considering the fuel cost, emission, voltage deviation and power losses using Multi-Objective Dragonfly algorithm," *Proceedings of the international conference on recent advances in electrical systems*, Tunisia, 2017, pp. 191-197.

BIOGRAPHIES OF AUTHORS






Mohammed Hamouda Ali    is a lecturer in Electrical Engineering Department at Al-Azhar University, Cairo, Egypt. He received his B.Eng., M.Eng. and Ph.D. degrees in Electrical Engineering from Al-Azhar University, Cairo, Egypt, in 2011, 2016, and 2021, respectively. His research interests are in power electronics, power system planning, optimization, operation, power system control, power quality, reliability, and renewable energy technology. He can be contacted at email: Eng_MohammedHamouda@azhar.edu.eg.



Ahmed Mohammed Attiya Soliman    has been a lecturer in Electrical Engineering Department at Al-Azhar University, Cairo, Egypt since 2018. He received his B.Sc., and M.Sc. Degrees from Al-Azhar University in 2008, and 2015 respectively; and a Ph.D. degree in Electrical Power Engineering from Al-Azhar University in 2018. He is interested in different fields like power electronics applications, high voltage direct current (HVDC) systems, electrical power quality, integration of renewable energy sources in electrical distribution networks, smart grids, and optimization techniques applications in electrical power system networks. He can be contacted at email: eng_ahmed1020@azhar.edu.eg.



Salah K. Elsayed    is an Associate professor at the Electrical Engineering Department- Faculty of Engineering- Al-Azhar University, Cairo-Egypt. He received his B.Sc., M.Sc. and Ph.D. Degrees from Al-Azhar University in 2005, 2009, and 2012 respectively. He is an Associate Prof. at the Electrical Engineering Department, College of Engineering, Taif University, Saudi Arabia. His areas of interest include Intelligent Systems Applications for Power Systems Stability and control. He can be contacted at email: salah_kamal1982@yahoo.com.